Journal of Chromatography A 1682 (2022) 463502

Contents lists available at ScienceDirect

Journal of Chromatography A

journal homepage: www.elsevier.com/locate/chroma

Ion mobility-mass spectrometry to extend analytical performance in the determination of ergot alkaloids in cereal samples

Laura Carbonell-Rozas[a,b], Maykel Hernández-Mesa[a,b,*], Laura Righetti[c], Fabrice Monteau[a], Francisco J. Lara[b], Laura Gámiz-Gracia[b], Bruno Le Bizec[a], Chiara Dall'Asta[c], Ana M. García-Campaña[b], Gaud Dervilly[a]

[a] Oniris, INRAE, LABERCA, 44300 Nantes, France
[b] Department of Analytical Chemistry, Faculty of Sciences, University of Granada, Campus Fuentenueva s/n, 18071 Granada, Spain
[c] Department of Food and Drug, University of Parma, Parco Area delle Scienze 17/A, 43124 Parma, Italy

ARTICLE INFO

Article history:
Received 28 July 2022
Revised 30 August 2022
Accepted 12 September 2022
Available online 14 September 2022

Keywords:
Ion mobility-mass spectrometry
Travelling wave ion mobility spectrometry
Ergot alkaloids
Cereal samples
Collision cross section

ABSTRACT

This work evaluates the potential of ion mobility spectrometry (IMS) to improve the analytical performance of current liquid chromatography-mass spectrometry (LC-MS) workflows applied to the determination of ergot alkaloids (EAs) in cereal samples. Collision cross section (CCS) values for EA epimers are reported for the first time to contribute to their unambiguous identification. Additionally, CCS values have been inter-laboratory cross-validated and compared with CCS values predicted by machine-learning models. Slight differences were observed in terms of CCS values for ergotamine, ergosine and ergocristine and their corresponding epimers (from 3.3 to 4%), being sufficient to achieve a satisfactory peak-to-peak resolution for their unequivocal identification. A LC-travelling wave ion mobility (TWIM)-MS method has been developed for the analysis of EAs in barley and wheat samples. Signal-to-noise ratio (S/N) was improved between 2.5 and 4-fold compared to the analog LC-TOF-MS method. The quality of the extracted ion chromatograms was also improved by using IMS.

1. Introduction

IMS has recently re-emerged as a powerful analytical separation technique due to the commercialization of the first hyphenated ion mobility-mass spectrometry (IM-MS) instrument in 2006 [1,2]. Since then, the interest in this technique has experienced an uninterrupted growth, and it has become popular in different scientific fields in which a great number of applications have been reported [3,4], especially related to *-omics* studies [5,6]. In addition, over the last years, the application of IM-MS in food analysis has increased considerably [7,8]. This trend is mainly due to the advantages offered by this technique when integrated into traditional analytical workflows based on liquid chromatography (LC), gas chromatography (GC) or capillary electrophoresis (CE) coupled to mass spectrometry (MS). It helps to address and overcome current challenges in the analytical field of food analysis [9]. Such challenges are associated with the complexity of food matrices, which contain a high number of compounds of different chemical nature. Food components vary significantly in their concentration, making it difficult to determine compounds at trace concentration levels. In this framework, the integration of IMS provides an additional separation dimension, thereby improving peak resolution. IMS is especially powerful to achieve the separation of isomeric and isobaric compounds [10,11]. Furthermore, the integration of IMS in LC-MS methods contributes to reduce the background noise, improves the S/N ratio and therefore, signal sensitivity, providing higher quality mass spectra for compound identification [12].

IMS is a gas-phase technique in which ionized molecules are separated based on their mobility in a carrier buffer gas through the drift tube (or mobility cell) under an electric field at atmospheric pressure or near to atmospheric pressure. The mobility of ions depends on their size, shape and charge. Thus, differences in these molecular characteristics lead to a faster or slower movement of the ions in the drift tube and allow their separation [13]. Typically, ion mobility is measured in terms of drift time, which corresponds to the time that the ions spend travelling through the

* Corresponding author at: LABERCA, University of Granada: Universidad de Granada, 101, route de Gachet, 44307 Nantes, Spain.
E-mail address: maykelhm@ugr.es (M. Hernández-Mesa).

https://doi.org/10.1016/j.chroma.2022.463502

mobility cell. Nevertheless, the drift time is an instrument dependent parameter, so the reporting of the so-called 'collision cross section' (CCS) is preferred to allow instrument comparison, as it is an intrinsic characteristic of each molecule [9]. CCS values can be obtained directly from drift time values by applying the Mason-Schamp equation in the case of drift tube ion mobility spectrometry (DTIMS) operating at low electric field [14]. When using other IMS technologies such as travelling wave ion mobility spectrometry (TWIMS) or trapped ion mobility spectrometry (TIMS), CCS measurements are only possible in systems calibrated with a specific mixture of compounds with known CCS [12]. The CCS parameter provides additional information to retention index and mass spectra, so it can be used as complementary identification parameter. As a consequence, a growing number of CCS databases have recently been created and are increasingly used for compound identification [6,15,16]. For example, the use of CCS values has been shown to provide more confidence in the determination of pesticide residues, reducing the reported false positive or negative assignments when LC multi-residue screening methods are assessed [17–19]. However, there is still a lack of CCS databases for food contaminants and residues; therefore, this parameter has not yet been fully implemented in food safety analysis and more research is needed in this context.

IMS appears as a powerful technique to improve the performance characteristics of non-targeted LC-MS methods. It has been recently applied in the analysis of residues and contaminants in feed and food-related matrices, as their analysis requires selective and sensitive analytical techniques [8]. Moreover, IMS allows the separation and isolation of targeted compounds from background noise and co-eluting matrix interferences in food samples. Due to the complexity of this sort of samples, the enhancement in signal sensitivity due to the integration of IMS can be very helpful to determine contaminants at trace levels [17,20]. However, to the date, this fact has hardly been exploited for this sort of samples [21,22]. Furthermore, most of the IMS-based methods developed in the food safety field have been focused on the analysis of pesticides, and few methods have been developed for the analysis of natural toxins in real samples [9]. IM-MS hyphenation was firstly investigated for the analysis of zearalerone in cornmeal [21], and recently, for the screening of multitoxins in fruits [22], achieving promising results in terms of S/N ratio and matrix interferences clean-up. In the last years, several studies addressing the CCS characterization of a large number of mycotoxins have been reported [23–25]. Nevertheless, ergot alkaloids (EAs) toxins, which are of special concern in food safety because of their relationship with the illness known as ergotism [26], have been scarcely studied by IM-MS [27].

EAs are indole secondary metabolites produced by all species of the *Claviceps* genus, most notably *C. purpurea*, which can parasitize over 600 plants including forage grasses and cereals, particularly rye, barley, wheat, and millet. Fungal parasitism begins in spring replacing the developing grain or seed with the ergot body or sclerotia containing about 0.15-0.5% of toxic alkaloids [26,28]. EAs have been detected in cereals and cereal products whose ingestion can cause human and animal poisoning [29,30]. The European Food Safety Authority (EFSA) has recommended paying special attention to ergometrine (Em), ergotamine (Et), ergosine (Es), ergocristine (Ecr), ergokryptine (Ekr), and ergocornine (Eco) and their corresponding epimers; ergometrinine (Emn), ergosinine (Esn), ergotaminine (Etn), ergocorninine (Econ), ergokryptinine (Ekrn) and ergocristinine (Ecrn), as they are the most predominant EAs (**Figure S1**) [31]. Due to concerns about the health risks that these compounds may pose in humans, the EFSA suggested a group acute reference dose of 1 μg kg^{-1} body weight and a group tolerable daily intake (TDI) of 0.6 μg kg^{-1} of body weight per day for the sum of the 12 main EAs [32]. The EFSA also stated that more analytical methods with the appropriate sensitivity and selectivity should be developed in order to reduce the uncertainty associated with the contamination of food and feed commodities with EAs [29]. Recently, with the Commission Regulation (EU) 2021/1399, a maximum of 200 mg kg^{-1} of ergot sclerotia has been set for unprocessed cereals (except for maize, rye and rice). In addition, maximum levels for EAs have been established for the first time in certain foodstuffs intended for human consumption, expressed as the sum of the main 12 EAs mentioned above [33]. The maximum contents allowed in milling products of barley, wheat, spelt and oats have been established in 100 or 150 μg kg^{-1} (depending on the ash content lower or higher than 900 mg/100 g, respectively). It is expected to fix the maximum content at 50 μg kg^{-1} from 2024. In the case of grains of these cereals placed on the market for the final consumer, the allowed content is 150 μg kg^{-1} and on the case of processed cereal-based food for children it is reduced to 20 μg kg^{-1}.

In the last years there has been an increase in the methods reported for the analysis of EAs in cereal and cereal-based food samples, mainly involving LC coupled to tandem mass spectrometry (MS/MS) [34–36]. However, unequivocal identification of major EAs is not easy due to the presence of epimers that exhibit the same accurate mass and lead to the same fragment ions. In addition, they tend to present similar retention times in LC separations (differences close to ±0.1 min), which can lead to their misidentification as they are often observed together in naturally contaminated samples. In view of these drawbacks, we hypothesized that the implementation of IMS can improve the performance characteristics of current LC-MS methods. Within this context, the aim of this work is to demonstrate for the first time the potential of using LC-IM-MS workflows for the analysis of EAs in cereal samples. For this purpose, the following studies were carried out: *(i)* characterization of travelling wave collision cross section against nitrogen buffer gas ($^{TW}CCS_{N_2}$) of EAs, including an inter-laboratory cross-validation; *(ii)* evaluation of the advantages, in terms of sensibility and selectivity, offered by the integration of TWIMS into a traditional LC-TOF-MS workflow; *(iii)* application of the proposed LC-TWIM-TOF-MS method to the determination of EAs in cereal samples.

2. Experimental

2.1. Chemicals and reagents

Standards of Es, Eco, Ekr, Ecr and the corresponding epimers, Esn, Econ, Ekrn, Ecrn, were purchased from Techno Spec (Barcelona, Spain), whereas Em, Et, Emn and Etn were obtained from Romer Labs (Getzersdorf, Austria). Dried standards were dissolved in acetonitrile (MeCN) to obtain stock standard solutions with concentrations of 500 μg mL^{-1} for the main EAs and of 125 μg mL^{-1} for the epimers. Immediately after their reconstitution, intermediate dried stock solutions were prepared by taking aliquots of individual or mixed standard solutions, which were placed into amber glass vials for their evaporation under a gentle stream of nitrogen. Finally, they were stored at -20 ºC to avoid EA epimerization and reconstituted in the required amount of MeCN just before use.

Methanol (MeOH), MeCN, and propan-2-ol (LC-MS Chromasolv® grade) were supplied by Sigma-Aldrich (St. Louis, Mo, USA). Water (HiperSolv Chromanorm® for HPLC) was provided by VWR International (West Chester, PA, USA). Formic acid (eluent additive for LC-MS) was acquired from LGC Standards GmbH (Wesel, Germany). Sodium hydroxide (1 M, Fisher Chemical™) and formic acid (Promochem®) were supplied by Fisher Scientific (Loughborough, UK) and LGC Standards (Wesel, Germany), respectively. Both were used for preparing a solution of sodium formate (0.5 mM in

90/10 (%, v/v) propan-2-ol/water), which was used for mass calibration. Dispersive sorbents used in the sample treatment procedure, namely Z-Sep+ and C18, were supplied by Supelco (Bellefonte, PA, USA) and Agilent Technologies (Madrid, Spain), respectively.

Leucine-enkephalin standard was acquired from Waters® (Manchester, UK) and used for the preparation of leucine-enkephalin (1 μg L^{-1}) in 50/50 (%, v/v) water/MeCN solution containing 0.2% (v/v) of formic acid. Leucine-enkephalin solution was used as a lock mass standard. A Major Mix IMS/TOF Calibration Kit from Waters® ref. 186008113 was used for CCS calibration.

In addition, for inter-laboratory studies, LC-MS grade MeOH and MeCN were purchased from Scharlab Italia S.r.l (Milan, Italy). Bi-distilled water was obtained using a Milli-Q System (Millipore, Bedford, MA, USA). Formic acid from Fisher Chemical (Thermo Fisher Scientific Inc., San Jose, CA, USA) was also used.

2.2. Instruments and equipment

A high-speed solid crusher (Hukoer, China), an evaporator System (System EVA-EC, from VLM GmbH, Bielefeld, Germany), a universal 320R centrifuge (Hettich Zentrifugen, Tuttlingen, Germany), a vortex-2 Genie (Scientific Industries, Bohemia, NY, USA), and a BenchMixer™ XL multi-tube vortexer (Sigma-Aldrich, St. Louis, MO, USA) were used for sample preparation.

Chromatographic separation was carried out in an Acquity UPLC® System from Waters® using an Agilent Zorbax Eclipse Plus RRHD C18 column (50 × 2.1 mm, 1.8 µm particle size). IM-MS analyses were performed on a hybrid quadrupole-TWIMS-orthogonal acceleration time-of-flight (TOF) mass spectrometer (Synapt G2-S HDMS, Waters®) equipped with an electrospray ionization (ESI) interface. These instruments are located at LABERCA (Nantes, France).

MassLynx (version 4.2, Waters®) software was used for data acquisition and DriftScope software (version 2.8), which is included in MassLynx software, was used to obtain data related to the CCS of ions and mobility spectra. Chromatograms were analyzed by SkyLine (version 21.1), which is an open-source software and allows processing mobility data as well as exploring the spectra produced by IMS-enabled mass spectrometers [37].

Inter-laboratory cross-validation of CCS values was carried out at the University of Parma (UNIPR, Italy). An ACQUITY I-Class UPLC separation system coupled to a Vion IMS-QTOF mass spectrometer (Waters®, Wilmslow, UK) equipped with an ESI interface was employed for $^{TW}CCS_{N_2}$ values cross-validation. Data acquisition was conducted using UNIFI 1.8 software (Waters®, Wilmslow, UK).

2.3. Sample preparation

The sample treatment used throughout this work was a modified QuEChERS procedure previously optimized to determine the 12 main EAs and their epimers in oat-based functional foods [38]. The description of the sampling of cereals, namely barley and wheat samples, has been already described in a previous work [39]. Briefly, a portion of 1.0 g of homogenized cereal samples was placed into a 50-mL falcon tube with conical bottom. Subsequently, the sample was mixed with 4 mL of the extraction mixture (MeCN:5 mM ammonium carbonate; 85:15, v/v). The sample was agitated by vortex for 1 min and centrifuged for 5 min at 9000 rpm and 4 ºC. The whole upper layer was collected and placed into a 15-mL falcon tube containing 150 mg of a mixture of C18:Z-Sep+ (1:1, w/w) as clean-up sorbent. Then, the mixture was vigorously shaken for 1 min and centrifuged for 5 min at 9000 rpm and 4 ºC. The entire upper layer was transferred to a 4 mL glass vial and the extraction solvent was evaporated to dryness under a gentle stream of nitrogen. Finally, the residue was reconstituted with 750 µL of a mixture of MeOH:ultrapure water (50:50, v/v) and filtered through a 0.22 µm nylon filter before injection.

2.4. Liquid chromatographic separation

A concentration gradient program was applied to achieve the chromatographic separation of 12 EAs. The mobile phase consisted of ultrapure water (eluent A) and MeOH (eluent B), both acidified with 0.3% (v/v) formic acid, and it was supplied at a flow rate of 0.4 mL min^{-1}. The eluent gradient profile was as follows: 0-2 min, 10% B; 2-4.5 min, 10-40% B; 4.5-9 min, 40-45% B; 9-11 min, 45-95% B; 11-12 min, 95% B; 12-13 min, 95-10% B. In order to guarantee column re-equilibration, initial conditions were maintained for 3 min, providing a total run time of 16 min. Column temperature was set at 35 °C and 5 μL was applied as injection volume. In order to avoid EAs epimerization, the duration of analysis sequences was limited to 12 hours and the temperature of the sample carrousel was kept at 10 °C during their execution.

For inter-laboratory cross-validation of CCS values, the separation conditions were similar to those mentioned above. Samples were injected (2 µL) and chromatographically separated using a reversed-phase C18 BEH ACQUITY column (50 × 2.1 mm, 1.7 µm particle size) from Waters® (Milford, MA, USA).

2.5. Ion mobility-mass spectrometry conditions

Analyses were performed in positive electrospray ionization (ESI+) mode, acquiring continuum data in the range of 50-1200 *m/z* with a scan time of 0.5 s. Leucine-enkephalin signal was acquired each 20 s for 0.3 s (3 scans to average). Nitrogen was used as both cone and desolvation gas at flow rates of 50 and 1000 L h^{-1}, respectively. Nebulizer pressure was fixed at 6.0 bar. Source and desolvation temperature were set at 150 °C and 350 °C, respectively. Capillary voltage was set at 3.0 kV, cone voltage at 31 V and source offset at 40 V. The TOF analyzer was operated in high-resolution mode for CCS characterization, and in sensitivity mode for the application of the LC-TWIM-TOF-MS method to the analysis of EAs in barley and wheat samples. Data acquisition was carried out using data independent $HDMS^E$, which is a data independent approach (DIA) involving IMS.

Regarding to IMS conditions, IMS buffer and trap gas consisted of nitrogen and were supplied at 90 and 0.4 mL min^{-1}, respectively. The flow rate of gas in the helium cell was 180 mL min^{-1}. IMS wave velocity and height were fixed at 1000 m s^{-1} and 40 V, respectively. In the trap cell, wave velocity and height were established at 311 m s^{-1} and 4.0 V, respectively. In the transfer cell, these parameters were set at 219 m s^{-1} and 4.0 V, respectively. Other HDMS settings were set as follows: trap DC bias, 47 V; and IMS DC bias, 3 V. CCS calibration was carried out using a Major Mix IMS/ToF Calibration Kit. CCS calibration covered the *m/z* range between 152-800 Da and a CCS range from 130.4 to 271 $Å^2$.

In the cross-validation of $^{TW}CCS_{N_2}$ values, IM-MS data were collected also in ESI+ mode over the mass range of 50−1000 *m/z*. Source settings were established as follows: capillary voltage, 1.0 kV; source temperature, 150 °C; desolvation temperature, 350 °C; and desolvation gas flow, 1000 L h^{-1}. The TOF analyzer was operated in sensitivity mode and data acquired using data independent $HDMS^E$. The optimized ion mobility settings were as follows: nitrogen flow rate, 90 mL min^{-1} (3.2 mbar); wave velocity, 650 m s^{-1}; and wave height, 40 V. CCS calibration using the same Major Mix IMS/TOF calibration kit (Waters®, Wilmslow, UK) was carried out covering the CCS range from 130 to 306 $Å^2$. The TOF was also calibrated prior to data acquisition and covered the *m/z* range from 151 to 1013 Da.

3. Results and discussion

3.1. CCS characterization

CCS characterization of all EAs has been carried out in positive ionization mode since these compounds are generally determined as their protonated form [35]. CCS values were measured using nitrogen as drift gas and reported following formalized nomenclature [40]. This study does not only provide information about the most abundant ion observed for each compound, but it also reports the $^{TW}CCS_{N_2}$ of all ions identified for each EA (i.e., $[M+H]^+$, $[M+Na]^+$ or $[M\text{-}H_2O+H]^+$), as well as the $^{TW}CCS_{N_2}$ for the main fragment ions measured. All detected ions were within a *m/z* range between 208 and 610 and presented $^{TW}CCS_{N_2}$ values between 139.9 and 241.8 Å^2. $^{TW}CCS_{N_2}$ measurements were carried out in triplicate and relative standard deviations (RSDs) lower than 0.5% were observed.

Detailed information of the investigated EAs, the ions observed, as well as their *m/z* and $^{TW}CCS_{N_2}$ can be found in Table 1. As can be seen, $[M+Na]^+$ ions can be used for the differentiation of the main compounds and their epimers, except in the case of Em and Emn because these ions were not observed when using the TWIMS instrument located at the UNIPR. This could be due to the different ion sources present in each instrument. In addition, only for Em and Emn, the $[M\text{-}H_2O+H]^+$ ions were not observed in any of the TWIMS platforms employed.

As previously reported, the CCS of ions is a molecular characteristic closely related to *m/z* [17,41]. Fig. 1 shows a general view of the correlation between both parameters for the main ions characterized in this work. As can be seen, all ions were located within a narrow interval (± 5%) from correlation curve (i.e., power regression model) represented as a solid line. A satisfactory correlation (R^2 = 0.9216) was obtained, showing that one single regression model is enough to describe the *m/z* and $^{TW}CCS_{N_2}$ relationship for all characterized ions. According to these results, ± 5% was observed as the interval of expected $^{TW}CCS_{N_2}$ for all the observed adducts. When several regression models are needed to explain such correlation, the obtained data could also provide interesting information for identifying the type of adduct formed in the ionization. This information can contribute to a more reliable assignment of molecular identities in non-targeted analysis [16]. Thus, the fact that one single regression model can describe the correlation between *m/z* and $^{TW}CCS_{N_2}$ means that all the observed ions and adducts present similar conformation in the gas phase. It limits the information offered by the $^{TW}CCS_{N_2}$ for the different types of ions observed for all EAs. Nevertheless, the $^{TW}CCS_{N_2}$ characterization of all ions of the same molecule observed during ionization provides complementary information that may contribute to peak grouping and further compound identification in non-targeted analysis [41].

As EAs have similar chemical structures, they show analogous fragmentation patterns and usually lead to the same fragment ions (i.e., *m/z* 208.1, 223.1, 268.1 and 305.1). $^{TW}CCS_{N_2}$ values for these major fragment ions are compared and represented in **Figure S2**. The results showed that similar $^{TW}CCS_{N_2}$ values were obtained for all fragment ions with the same *m/z* regardless the molecular ion from which they were originated. This is due to the fact that these

Table 1
$^{TW}CCS_{N_2}$ database for EAs. Cross-validation of $^{TW}CCS_{N_2}$ values and comparison with the values obtained by machine-learning approaches.

EA	Ions	*m/z*	$^{TW}CCS_{N_2}$ LABERCA (n = 3)*	%RSD (n = 3)	$^{TW}CCS_{N_2}$ UNIPR (n = 3)**	%RSD (n = 3)	inter-lab Bias (%)	Hines et al. [63]	machine-learning approaches			
									CCS base [64]	Bias%	All CCS [65]	Bias%
Em	$[M+H]^+$	326.1868	181.1	0.02	181.1	0.16	0.00	179.0	177.1	-2.21	179.7	-0.77
	$[M\text{-}H_2O+H]^+$	307.1684	-	-	-	-	-				176.7	
	$[M+Na]^+$	348.1687	186.9	0.01	-	-	-		184.2	-1.44	183.3	-1.93
Emn	$[M+H]^+$	326.1868	182.1	0.05	181.7	0.09	-0.25		177.1	-2.75	179.7	-1.32
	$[M\text{-}H_2O+H]^+$	307.1684	-	-	-	-	-		-		176.7	
	$[M+Na]^+$	348.1687	189.2	0.09	-	-	-		184.2	-2.64	183.3	-3.12
	$[M+H]^+$	548.2872	234.2	0.02	234.0	0.49	-0.01		229.2	-2.13	227.6	-2.82
Es	$[M\text{-}H_2O+H]^+$	530.2767	214.9	0.01	228.0	0.41	6.10		-		226.3	5.30
	$[M+Na]+$	570.2692	234.2	0.07	232.3	0.26	0.83		230.9	-1.41	229.0	-2.22
	$[M+H]^+$	548.2872	231.3	0.01	232.5	0.28	0.49		229.2	-0.91	227.6	-1.60
Esn	$[M\text{-}H_2O+H]^+$	530.2767	222.2	0.01	224.7	0.13	1.12		-		226.3	1.85
	$[M+Na]^+$	570.2692	226.5	0.04	225.1	0.15	-0.60		230.9	1.94	229.0	1.10
	$[M+H]^+$	582.2716	236.0	0.03	236.8	0.31	0.35	231.8	235.5	-0.21	235.1	-0.38
Et	$[M\text{-}H_2O+H]^+$	564.2610	222.7	0.01	-	-	-		-		234.1	5.12
	$[M+Na]^+$	604.2535	236.3	0.02	235.8	0.41	0.23		239.3	1.27	236.4	0,04
	$[M+H]^+$	582.2716	234.9	0.01	234.3	0.05	-0.27		235.5	0.26	235.1	0,09
Etn	$[M\text{-}H_2O+H]^+$	564.2610	224.6	0.04	227.6	0.09	1.31		-		234.1	4.23
	$[M+Na]+$	604.2535	227.2	0.01	226.7	0.09	-0.23		239.3	5.33	236.4	4.05
	$[M+H]^+$	562.3029	236.3	0.06	236.6	0.19	0.11		232.3	-1.69	230.0	-2.67
Eco	$[M\text{-}H_2O+H]^+$	544.2923	220.4	0.03	230.6	0.32	4.64		-		228.8	3.81
	$[M+Na]^+$	584.2848	235.9	0.14	234.4	0.03	-0.63		233.5	-1.02	231.4	-1.91
	$[M+H]^+$	562.3029	235.2	0.01	237.2	0.01	0.88		232.3	-1.23	230.0	-2.21
Econ	$[M\text{-}H_2O+H]^+$	544.2923	224.9	0.02	229.5	0.09	2.04		-		228.8	1.73
	$[M+Na]^+$	584.2848	233.1	0.09	233.1	0.87	0.01		233.5	0.17	231.4	-0.73
	$[M+H]^+$	576.3185	239.5	0.32	240.4	0.41	0.40	236.1	236.0	-1.46	233.5	-2.51
Ekr	$[M\text{-}H_2O+H]^+$	558.3080	222.7	0.44	-	-	-		-		232.3	4.31
	$[M+Na]^+$	598.3005	239.1	0.32	238.6	0.08	-0.23		236.8	-0.96	234.8	-1.80
	$[M+H]^+$	576.3185	239.2	0.02	241.6	0.23	0.99		236.0	-1.34	233.5	-2.38
Ekrn	$[M\text{-}H_2O+H]^+$	558.3080	231.1	0.11	234.1	0.02	1.30		-		232.3	0.52
	$[M+Na]^+$	598.3005	233.7	0.05	232.0	0.15	-0.71		236.8	1.33	234.8	0.47
	$[M+H]^+$	610.3029	242.7	0.06	243.6	0.33	0.38		242.3	-0.16	241.5	-0.49
Ecr	$[M\text{-}H_2O+H]^+$	592.2923	231.2	0.01	234.6	0.45	1.47		-		240.6	4.07
	$[M+Na]+$	632.2848	241.7	0.03	240.4	0.47	-0.53		245.1	1.41	242.6	0.37
	$[M+H]+$	610.3029	241.4	0.01	243.3	0.10	0.79		242.3	0.37	241.5	0.04
Ecrn	$[M\text{-}H_2O+H]^+$	592.2923	233.9	0.05	237.0	0.02	1.31		-		240.6	2.86
	$[M+Na]^+$	632.2848	233.9	0.05	233.7	0.16	-0.09		245.1	4.79	242.6	3.72

* $^{TW}CCS_{N_2}$ database was generated at LABERCA.
** $^{TW}CCS_{N_2}$ cross-validation was carried out at UNIPR.

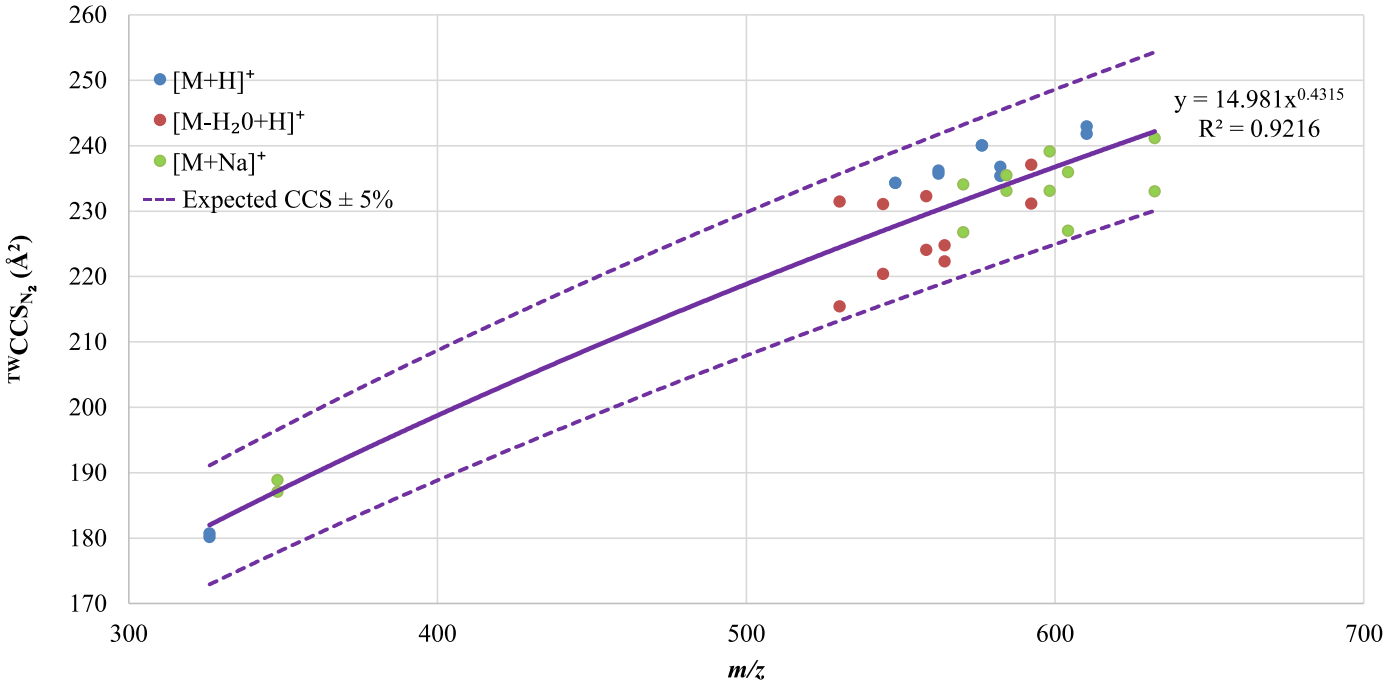

Fig. 1. Representation of CCS vs *m/z* for the main ions characterized.

molecules do not conserve their isomeric properties after fragmentation. This results in identical fragment ions for the different EAs and therefore the same $^{TW}CCS_{N_2}$ values for said ion fragments. In this regard, CCS values for fragment ions cannot offer additional information for the determination of EAs. Nevertheless, the development of a $^{TW}CCS_{N_2}$ database for fragment ions may help the recognition and identification in non-targeted approaches of unknown EAs so far.

The aim of reporting $^{TW}CCS_{N_2}$ values for major EAs and their epimers is to support their determination and reduce the number of false positives found when applying classical LC-MS workflows. This contributes to develop methods for targeted analysis with high selectivity and supporting molecular identification in non-targeted analysis. This strategy has been already successfully applied for unambiguous identification of targeted pesticides in food samples [19]. In this sense, in order to use $^{TW}CCS_{N_2}$ values in the determination of EAs with high confidence, experimental $^{TW}CCS_{N_2}$ values must be cross-validated, either experimentally by external laboratories or by means of computational calculations or machine-learning predictions.

3.1.1. Cross-validation of the $^{TW}CCS_{N_2}$ values of EAs

The challenges associated with reporting CCS values are to demonstrate that they can be used as reference values in other laboratories equipped with the same IMS technology used to obtain the CCS values in the first instance [42], as well as on IMS platforms based on different IMS technology [43]. In this context, the cross-validation of the $^{TW}CCS_{N_2}$ values for EAs reported in this work was carried out by an external laboratory located at the University of Parma (Italy). This laboratory is equipped with a different TWIMS platform than the one employed at LABERCA (i.e., Synapt G2-S vs Vion). Therefore, this cross-validation study also evaluates whether $^{TW}CCS_{N_2}$ values can be transferred within laboratories equipped with different TWIMS platforms.

EA standard mixtures prepared at different concentration levels, specifically at 50, 100, and 250 μg L^{-1}, were analyzed in triplicate. Therefore, $^{TW}CCS_{N_2}$ values were the result of nine measurements (Table 1). RSDs below 0.9% were observed for the $^{TW}CCS_{N_2}$ measurement of protonated ions and sodium adducts. Only few ions such as $[M+Na]^+$ ions of Em and Emn and $[M-H_2O+H]^+$ of Et and Ekr were not detected by the Vion IMS instrument at UNIPR, which is generally due to the fact that ion formation depends on the instrumental configuration and ionization conditions, so different ions can be generated. In the case of $[M-H_2O+H]^+$ ions, the RSD obtained was below 2% for most analytes, except for Esn, Eco and Econ. Regarding CCS deviation between UNIPR and LABERCA laboratories, the bias was below 1% in all cases except for the $[M-H_2O+H]^+$ ions of Esn, Eco and Econ. The correlation between the $^{TW}CCS_{N_2}$ values generated by both laboratories for the main characterized ions is shown in **Figure S3.** High correlation coefficients (r) of 0.9895 and 0.9992 were obtained for $[M+H]^+$ and $[M+Na]^+$ ions, respectively. These data indicated a strong linear relationship between the CCS values generated by both IMS platforms. In the case of $[M-H_2O+H]^+$ ions, the correlation coefficient was lower (r=0.7909), although still acceptable since it is above 0.7.

To sum up, 73.3% of the $^{TW}CCS_{N_2}$ values of ions detected by both TWIMS platforms showed a bias below 1%, and for 90% of $^{TW}CCS_{N_2}$ values this was below 2%. This is in accordance with the widely accepted 2% bias threshold for CCS measurements in TWIMS and commonly used for molecular identification based on CCS values [6,8,18]. These results confirm that the $^{TW}CCS_{N_2}$ values for EAs have been successfully cross-validated by an external laboratory, particularly the $^{TW}CCS_{N_2}$ values for $[M+H]^+$ and $[M+Na]^+$ ions. Therefore, these $^{TW}CCS_{N_2}$ values can be used in studies involving the identification of EAs and carried out by laboratories equipped with TWIMS technology. However, in the case of $[M-H_2O+H]^+$ ions, further investigation is necessary to understand the bias existing between the values obtained by both TWIMS instruments.

3.1.2. Machine-learning approach

Traditionally, CCS values have been obtained through the experimental measurement of chemical standards or using computational modeling [44,45]. However, these strategies have some limitations. In the case of experimental measurements, there is

a limited availability of chemical standards, whereas the choice of a suitable calibrant with similar structure to the target analytes for calibrant-dependent methods (e.g., TWIMS methods) determines the accuracy of the experimental CCS data obtained [40]. On the other hand, computational modeling is computationally intensive and is likely to produce large error, especially in molecules with flexible structures [46]. In this context, machine-learning approaches have recently emerged as predictive tools to produce CCS values on a large scale. The prediction principle is based on the use of a training dataset through which the machine-learning algorithm learns the relationship between molecular descriptors and their experimental CCS values (training data). A prediction model is then established and allows CCS values to be rapidly predicted. Finally, the external validation dataset is used to validate and evaluate the prediction error [47]. This methodology has already been implemented to generate the CCS values for the identification of small molecules [48,49], presenting a low prediction error (around 1-3%) and being more computationally efficient compared to computational modeling [47]. Recently, different platforms based on machine-learning models, such as CCSbase [50] and AllCCS [51], have been developed to complement CCS experimental data. These platforms provide predicted CCS values for target compounds taking into consideration their molecular descriptors such as the simplified molecular-input line-entry system (SMILE) for describing the structure of the molecule or their accurate mass. In addition, in the absence of experimental or library CCS data, CCS predictions can help to reduce analysis time in identification approaches since they reduce the number of potential candidates [52].

In this work, CCSbase and AllCCS web servers were used to compare the predictive CCS values with the experimental $^{TW}CCS_{N_2}$ values obtained for EAs using TWIMS, as shown in Table 1. While CCSbase model provided CCS data for $[M+H]^+$ and $[M+Na]^+$ ions, but not for $[M-H_2O+H]^+$ ions, AllCCS tool provided information for all three types of ions. The results obtained by the machine-learning web servers showed a prediction error within 5% for 94.8% of all $^{TW}CCS_{N_2}$ values previously obtained experimentally, and within 3% for 93.8% of all CCS values corresponding to $[M+H]^+$ and $[M+Na]^+$ ions, resulting in a median relative error below 1.9%. These results are in the same range as previously reported prediction errors for CCS values machine-learning approaches [48,49]. The CCS values with a higher bias compared to the $^{TW}CCS_{N_2}$ values corresponded to $[M-H_2O+H]^+$ ions as it was also noticed in the CCS cross-validation study.

Although these prediction error values were considered satisfactory, the bias between the CCS values obtained experimentally and the CCS values predicted by machine-learning models could be reduced by feeding these models with more experimental data. Overall, due to the lack of CCS databases including EAs, the machine-learning based prediction is a useful and user-friendly option to generate CCS values for uncharacterized EAs, as well as to offer more confidence to experimentally generated CCS values.

3.2. Selectivity enhancement by ion mobility spectrometry

TWIMS offers a third separation dimension to LC-MS workflows in which the compounds can be separated according to their CCS. Molecules that are more compact interact to a lesser degree with the buffer gas than elongated molecules, thus they traverse the drift cell in shorter times. Therefore, this molecular characteristic can be used to achieve the separation of analytes that co-elute in the chromatographic dimension and/or molecules with similar or identical *m/z* [3,53]. In this sense, slight differences between the $^{TW}CCS_{N_2}$ values of compounds with similar or equal *m/z,* as is the case of the main EAs and their epimers, may be enough to separate and distinguish them. As theoretically suggested, CCS differences of about 2% should be enough for identification purposes (peak-to-peak resolution), while more than 5% is likely required for quantification (baseline resolution) [54]. On this basis, sodium adducts of Et ($^{TW}CCS_{N_2}$ = 236.3 Å^2) and its epimer Etn ($^{TW}CCS_{N_2}$ = 227.2 Å^2) could be at least peak-to-peak separated by TWIMS since the CCS difference between them was higher than 2% (i.e., 4%). Similarly, sodium adducts of Es ($^{TW}CCS_{N_2}$ = 234.2 Å^2) and its epimer Esn ($^{TW}CCS_{N_2}$ = 226.5 Å^2) presented a difference of 3.4% and also sodium adducts of Ecr ($^{TW}CCS_{N_2}$ = 241.7 Å^2) and its epimer Ecrn ($^{TW}CCS_{N_2}$ = 233.9 Å^2) with a CCS difference of 3.3%. As shown in Fig. 2, partial separation was achieved between Etn-Et, Esn-Es and Ecrn-Ecr, which is enough for the differentiation of epimers and is in agreement with the observed differences in CCS values and the maximum expected peak resolution of the Synapt system. Despite the fact that the epimers were not fully separated to baseline, these results highlight the potential of TWIMS as a complementary dimension for improving EA separation and method selectivity in traditional LC-MS workflows. Since the differences in retention times of EAs provided by LC-MS methods are close to ±0.1 min, the differences in the $^{TW}CCS_{N_2}$ values would be very useful to distinguish them in order to avoid their misidentification and also the possible reporting of false positive/negative samples.

Moreover, taking into account these results, and that new IMS technologies such as cyclic ion mobility spectrometry (cIMS) which presents an increased separation resolution [55], these ion pairs could be baseline separated by IMS.

In addition, the integration of IMS in LC-MS methods allows the separation of target compounds from matrix interferences that present similar retention times and *m/z*. This leads to an enhancement in selectivity, which is essential for peak integration and quantification of target compounds. This improvement has been previously demonstrated in the food safety field for the determination of zearalerone and its metabolites [21], β-agonists [56], and steroid isomers [57]. To investigate this advantage for the determination of EAs in cereals, barley samples were treated following a QuEChERS protocol. Subsequently, the extracts were analyzed by LC-TWIM-TOF-MS. Extracted ion chromatograms (EICs) obtained using TWIMS as third separation dimension were compared with those obtained without applying this additional separation dimension. As can be seen in Fig. 3, Em co-eluted with several matrix compounds with *m/z* 326.2, making peak integration impossible. However, when the drift time range of the protonated molecule of Em was selected as signal filter, these matrix compounds were removed from the EICs, allowing the effective integration of Em peak. Thus, the application of IMS allowed the isolation of this analyte from matrix interferences, granting its unequivocal identification and chromatographic integration.

Another example of improving selectivity by using TWIMS is the case of Ekr and Ekrn. Both analytes co-eluted with matrix interferences that, although they showed a low signal sensitivity, were integrated with the chromatographic peaks of Ekr and Ekm (Fig. 4). This could lead to erroneous conclusions about the analyte concentration in the sample or even a false positive. However, selecting the drift time range of the protonated molecule for both analytes, these matrix compounds were removed from the EIC.

These results show how TWIMS allows the isolation of the analytes of interest form the chemical background of the matrix, improving method selectivity. Additionally, this has a major impact on the quality of MS spectra, as cleaner MS spectra are obtained when TWIMS is integrated into the analytical workflow. This is of especial interest for the determination of chemical residues and contaminants at trace levels in complex matrices composed by a high number of compounds such as food samples, as it has been reported for the determination of mycotoxins in cornmeal [21] or fruits [20]. Therefore, the implementation of TWIMS can provide more reliable results not only for quantification purposes, but also

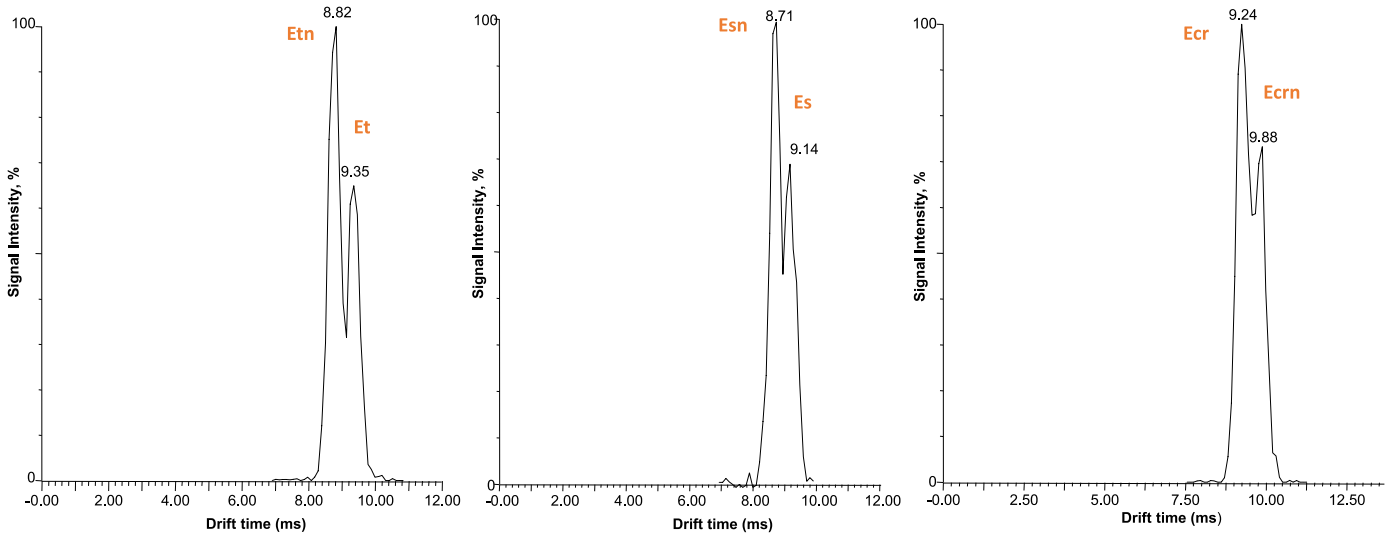

Fig. 2. Mobility spectra for the separation of sodium adducts of: a) Et and Etn; b) Es and Esn; c) Ecr and Ecrn by TWIMS. Mobility spectra have been obtained after applying the following signal filters: a) *m/z* 604, Rt between 3.8 and 4.3 min, and drift time between 7 and 11 ms; b) *m/z* 570, Rt between 3.2 and 3.9 min, and drift time between 7 and 9 ms; c) *m/z* 632, Rt between 6.0 and 8.2 min, and drift time between 7.5 and 11 ms.

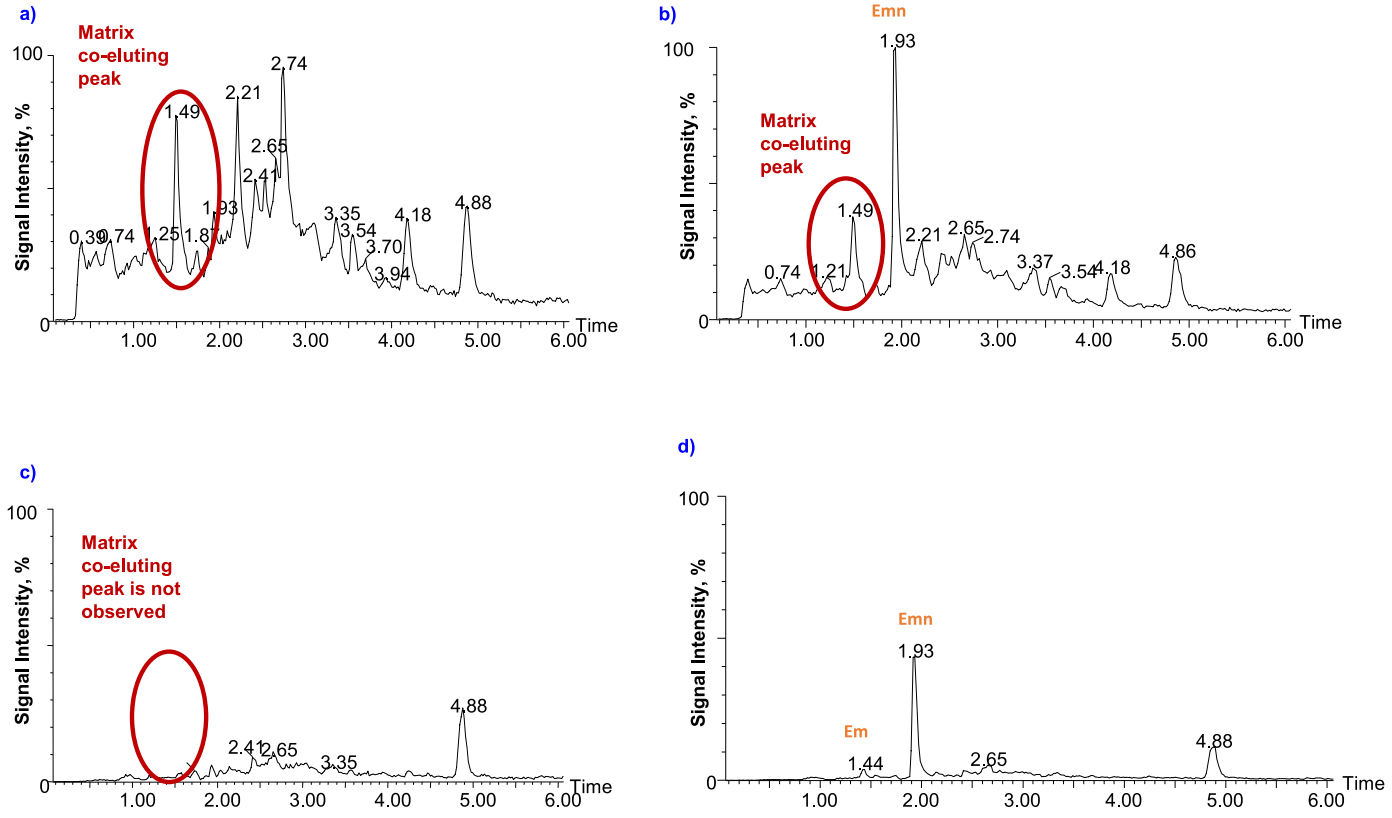

Fig. 3. EICs (*m/z* 326.2) resulted from the analysis of: a) and c) non-spiked barley samples, and b) and d) barley samples spiked with EAs (5 μg kg^{-1}; $[M+H]^+$). Analyses were performed by LC-ESI-TWIM-TOF-MS in positive mode. In c) and d), the mobility region of the protonated molecule of Em (i.e between 52 and 62 ms) was selected.

for identification purposes (i.e. cleaner MS spectra in addition to the ^{TW}CCS parameter).

3.3. Sensitivity enhancement by ion mobility spectrometry

In addition to the selectivity enhancement achieved using IMS in LC-MS workflows, an improvement in signal sensitivity can also be achieved [9]. Due to the isolation of the analyte from the chemical background of the matrix discussed in the previous section, the limits of detection (LODs) of the method can be reduced significantly. In this work, the benefit of using TWIMS was also investigated for the determination of EAs in barley samples. As can be seen in Fig. 5, and discussed in Section 3.2, cleaner EICs were observed when the drift time range was used as signal filter; thus, it facilitates peak integration of EAs and improves S/N ratio. The S/N ratio was generally improved between 2.5 and 4 times when the drift time range of target analytes was selected as signal filter. For all studied EAs, except for Ekr and Ekrn, the analytical signal

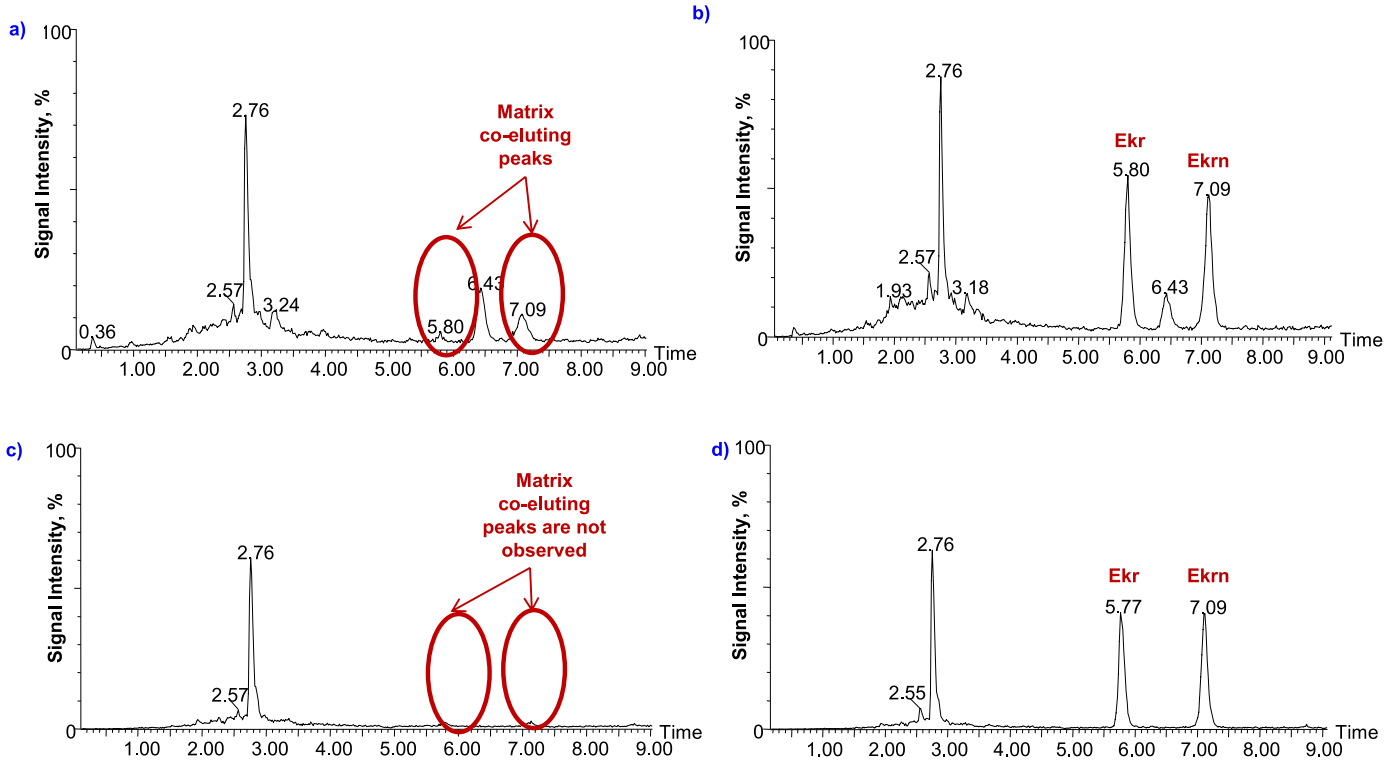

Fig. 4. EICs (*m/z* 576.3) resulted from the analysis of: a) and c) non-spiked barley samples, and b) and d) barley samples spiked with EAs (5 μg kg^{-1}; $[M+H]^+$). Analyses were performed by LC-ESI-TWIM-TOF-MS in positive mode. In c) and d), the mobility region of the protonated molecule of Ekr (i.e between 107 and 87 ms) was selected.

observed at a concentration level of 5 μg kg^{-1} was below the limit of quantification (LOQ, S/N=10) without applying this filter. However, when the drift time range of these compounds was selected as signal filter, the observed analytical signal was above the LOQ. As consequence, their quantification at this concentration level was only possible when the mobility spectra was also explored for data processing.

Additional studies were carried out to evaluate the signal sensitivity provided by the LC-TWIM-MS method compared to the traditional LC-MS method. Blank barley samples (n = 2) were spiked at 25 μg kg^{-1} and treated according to the QuEChERS protocol. Subsequently, the extracts were injected and analyzed by LC-ESI-TWIM-TOF-MS and LC-ESI-TOF-MS in positive mode using the same LC and ESI conditions in both methods. The TOF system was operated in sensitivity mode to improve signal sensitivity. Although a lack of sensitivity is usually attributed to IM-MS methods, signal sensitivity was not significantly decreased when EAs were analyzed by LC-IMS-MS in comparison to the results obtained by LC-MS (**Figure S4**). This shows that in recent years there have been notable instrumental improvements that have made it possible to overcome the low ion transmission typically associated with IMS systems, which is the reason why IMS was considered a low sensitivity technique for a long time [3].

In short, our results show the benefits, in terms of signal sensitivity, of integrating TWIMS into a LC-MS workflow for EAs determination, which is reflected in the reduction of background noise and the increase of the S/N ratio.

3.4. Application of ion mobility spectrometry to determine EAs in cereal samples

The proposed QuEChERS-LC-ESI-TWIM-TOF-MS method was characterized in terms of linearity, LODs, LOQs, and precision in cereal samples. Firstly, procedural calibration curves for barley and wheat samples were prepared by spiking blank samples of each matrix at six different concentration levels (2, 5, 10, 25, 50 and 100 $\mu g\ kg^{-1}$). Two samples per each concentration level were processed according to the QuEChERS procedure and analyzed in duplicate. Peak area was considered as a function of the analyte concentration. LODs and LOQs were calculated as the minimum analyte concentration with S/N equal to 3 and 10, respectively. The statistical parameters calculated by least-square regression, as well as LODs and LOQs, are shown in Table 2. Data treatment was carried using the software SkyLine in which, apart from the major transitions and retention times, the data can be also filtered taking into consideration the drift time and the CCS of each compound.

Although a limited dynamic range is typically associated with LC-IM-MS methods compared to LC-MS methods [58], the same dynamic linear range (2 – 100 $\mu g\ kg^{-1}$) was observed for the determination of EAs in cereals when the samples were analyzed by both LC-TWIM-MS and LC-MS. In general, a satisfactory linearity was achieved for the determination of EAs in both samples (R^2 > 0.99) in the concentration range studied. LOQs ranged between 0.7 and 2.0 $\mu g\ kg^{-1}$ for the determination of EAs in barley samples, and between 0.7 and 2.1 $\mu g\ kg^{-1}$ for EAs in wheat samples. These LOQs are comparable to and even lower than those obtained by LC-triple quadrupole (QqQ)-MS for the determination of EAs in similar samples [39,59,60].

According to SANTE/12682/2019 guideline, one representative sample can be selected from a commodity group for the validation of the method [61]. Since barley and wheat are included in the same group, barley samples were chosen as representative commodity for the precision study. Precision was evaluated in terms of repeatability (intra-day precision) and intermediate precision (inter-day precision) by the application of the proposed QuEChERS-LC-ESI-TWIM-TOF-MS method to barley samples spiked at two concentration levels of the linear range (i.e. 5 and 50 $\mu g\ kg^{-1}$). For repeatability studies, two samples fortified at

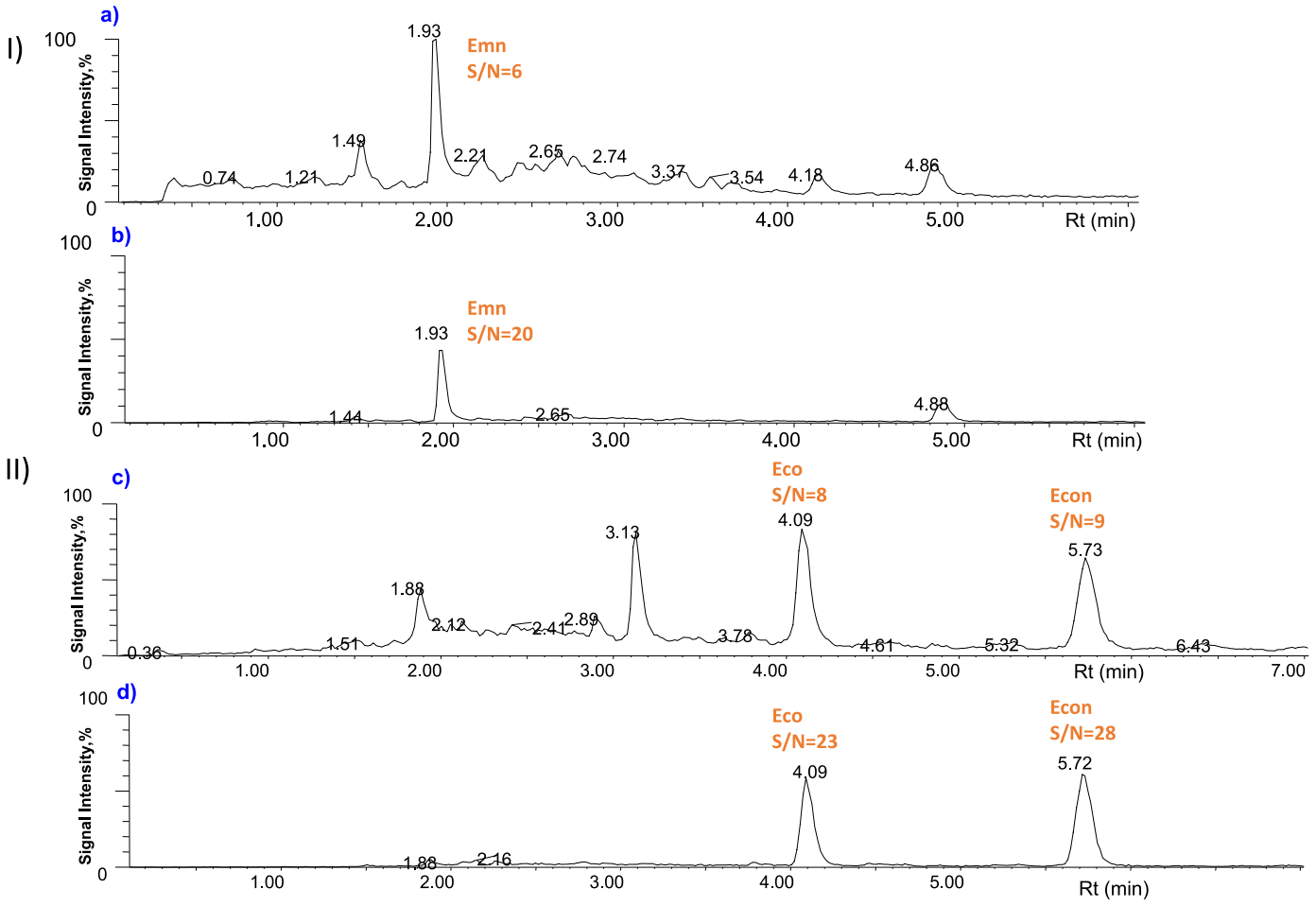

Fig. 5. EICs resulted from the analysis of: I) Emn (5 μg kg^{-1}; $[M+H]^+$) and II) Eco and Econ (5 μg kg^{-1}; $[M+H]^+$) in barley samples by LC-ESI-TWIM-TOF-MS in positive mode. The following filters were applied for signal processing of related total ion chromatograms: a) *m/z* 362.2; b) *m/z* 362.2 and drift time range between 52-62 ms; c) *m/z* 562.3; d) *m/z* 562.3 and drift time range between 87-103 ms.

Table 2
Statistical and performance characteristics of the proposed method for the determination of the main EAs and their epimers in barley and wheat samples.

	BARLEY				WHEAT			
EA	Linear regression equation	R^2	LOD (μg kg^{-1})	LOQ (μg kg^{-1})	Linear regression equation	R^2	LOD (μg kg^{-1})	LOQ (μg kg^{-1})
Em	y=148.58x-383.66	0.9909	0.6	2.0	y=61.207x-234.38	0.9907	0.5	1.6
Emn	y=2140.8x-5747.6	0.9925	0.3	0.9	y=1594.7x-5443.6	0.9920	0.2	0.7
Esn	y=2417.4x-6711.9	0.9914	0.3	1.1	y=417.73x-2083.7	0.9903	0.6	2.0
Es	y=1524.2x-5618.8	0.9925	0.4	1.3	y=503.26x-3227.1	0.9902	0.5	1.7
Etn	y=2565.2x-7002	0.9909	0.3	0.9	y=573.41x-2633.8	0.9914	0.3	0.8
Eco	y=5267.2x-13521	0.9943	0.2	0.7	y=3453.6x-15732	0.9910	0.3	0.9
Et	y=5154.3x-11715	0.9944	0.2	0.8	y=3374.6x-16568	0.9912	0.2	0.7
Econ	y=4090.1x-13377	0.9911	0.3	0.9	y=1898.1x-9306.5	0.9935	0.5	1.5
Ekr	y=3748.3x-10774	0.9923	0.2	0.6	y= 2099.3x-11451	0.9910	0.3	1.1
Ecr	y=1727.5x-4664.2	0.9906	0.3	0.9	y=418.85x-971.83	0.9925	0.4	1.3
Ekrn	y=3711.8x-14007	0.9906	0.4	1.3	y=685.41x-4182.1	0.9902	0.6	2.0
Ecrn	y=2185x-6172.2	0.9913	0.3	1.0	y=1325.3x-5369.6	0.9939	0.2	0.7

each concentration level were submitted to sample treatment and injected in triplicate on the same day under the same conditions. Intermediate precision was evaluated with a similar procedure but analyzing one spiked sample in triplicate and per day for three different days. The obtained results, expressed as relative standard deviation (RSD, %) of peak areas, are summarized in Table 3. RSD values lower than 14.4% were obtained in all cases. This agrees with the EU recommendations for the performance of analytical methods, which set an upper limit for RSD of 20% [62].

In addition, in order to demonstrate the applicability of the method, contaminated cereal samples from Algeria previously analyzed by UHPLC-MS/MS [39] were also investigated using the proposed method. In this previous work eight samples of wheat and four samples of barley were found to contain EAs, with Ekr and Ecr in wheat and Em in barley being the most frequent EA contamination. These samples were subsequently analyzed by LC-ESI-TWIM-TOF-MS. The results obtained by the analysis of contaminated barley and wheat samples are shown in **Tables S1** and **S2**, respectively. Em and its epimer Emn were the most common EAs

Table 3
Precision of the proposed method for the determination of the main EAs and their epimers in spiked barley samples.

	Repeatability, %RSD (n = 6)		Intermediate precision, %RSD (n = 9)	
	5 μg kg^{-1}	50 μg kg^{-1}	5 μg kg^{-1}	50 μg kg^{-1}
Em	9.3	6.5	13.6	8.5
Emn	8.0	5.0	12.9	6.3
Esn	11.0	6.2	11.3	9.6
Es	8.5	6.8	12.9	7.4
Etn	9.8	4.6	10.2	7.7
Eco	13.0	8.8	9.2	6.6
Et	7.8	5.6	11.7	9.4
Econ	7.3	6.6	11.5	7.8
Ekr	9.5	7.1	14.4	9.4
Ecr	8.1	5.9	9.0	7.5
Ekrn	10.5	8.7	9.9	8.0
Ecrn	5.3	7.5	8.7	6.6

found in barley samples, while Ekr and Ecr showed the highest incidences in wheat. The total EA concentration ranged between 8.3 and 36.8 μg kg^{-1} for barley samples and between 5.2 and 65.0 μg kg^{-1} for wheat samples. These total contents are below the maximum level for EAs of 150 μg kg^{-1} set for barley and wheat grains placed on the market for the final consumer [33].

It was observed that the majority of the EAs determined in both samples matched with the incidence of EAs reported previously by applying the UHPLC-MS/MS method [39]. In this previous work, total content of EAs was found to be in the range of 17.8 to 53.9 μg kg^{-1} for the same barley samples, and in the range of 3.66 to 76.0 μg kg^{-1} for wheat samples. It is worth mentioning that Em was found in higher concentrations than the rest of the EAs, reaching a maximum concentration of 25 μg kg^{-1} and 50 μg kg^{-1} in wheat and barley samples, respectively. These results are in agreement with the levels of EAs found in the present study. Obviously, the samples have been analyzed at different time intervals, so the time and storage conditions of the samples may have influenced the accuracy of the results of both studies. Likewise, it should be noted that Emn was found in the LOD-LOQ range and was not quantified when the barley samples were analyzed by UHPLC-MS/MS. However, due to the implementation of TWIMS in the LC-MS workflow and taking into account the S/N improvement achieved for Emn (Fig. 5), this analyte could be quantified by LC-ESI-TWIM-TOF-MS.

4. Conclusions

The present work shows the advantages provided by the integration of IMS into LC-MS workflows focused on EA determination. These advantages mainly lead to higher separation resolution and higher confidence in analyte identification. In this regard, $^{TW}CCS_{N_2}$ values for the main EAs and their epimers are reported for the first time. This parameter is complementary to *m/z* and retention times, and useful for the identification of these compounds, especially in non-targeted analysis. $^{TW}CCS_{N_2}$ values were successfully inter-laboratory cross-validated with satisfactory bias (< 2%). Furthermore, the advantages provided by the implementation of TWIMS in LC-MS workflows, in terms of selectivity and sensitivity, have been demonstrated in cereal samples. The separation of sodium adducts of Et, Es and Ecr and their corresponding epimers, as well as, the separation of EAs from matrix interferences, demonstrate the selectivity enhancement provided by TWIMS in food safety applications. TWIMS has also been an effective tool for reducing background noise, improving the S/N ratio for the studied compounds in cereal samples between 2.5 and 4 times and, consequently, enhancing the sensitivity of the method. In addition, a QuEChERS-LC-TWIM-TOF-MS method has been applied to the determination of EAs in barley and wheat samples previously reported as contaminated samples. In this regard, the use of IMS has been effective to reduce the number of possible false results of EAs in such samples.

Therefore, IMS is a powerful technique for enhancing the performance characteristics of LC-MS methods destined to the analysis of contaminants in food and food-related matrices. However, more research involving its application to answer food safety issues is needed to truly implement this analytical tool in this field. In this regard, there are some drawbacks such as that the regulation on the performance of analytical methods does not yet propose the inclusion of the IMS as separation technique or that its standardization (e.g. with guidelines, data standards and reporting) is not yet completed. Furthermore, data processing software packages are required since automated signal peak detection for multidimensional data files (*m/z*, Rt, CCS) is currently not possible with MS suppliers softwares. In the same way, the deconvolution over all dimensions to group peaks into their chemical components particularly important in non-target workflows is not feasible. Therefore, the integration of IMS in current LC-MS workflows involves certain challenges, especially in food analysis where this technique is still in development.

Declaration of Competing Interest

The authors declare that they have no known competing financial interests or personal relationships that could have appeared to influence the work reported in this paper.

CRediT authorship contribution statement

Laura Carbonell-Rozas: Formal analysis, Investigation, Writing – original draft. **Maykel Hernández-Mesa:** Conceptualization, Methodology, Supervision, Writing – review & editing, Project administration. **Laura Righetti:** Investigation, Methodology, Supervision, Writing – review & editing. **Fabrice Monteau:** Resources. **Francisco J. Lara:** Supervision, Writing – review & editing. **Laura Gámiz-Gracia:** Supervision, Writing – review & editing. **Bruno Le Bizec:** Conceptualization, Project administration, Funding acquisition. **Chiara Dall'Asta:** Supervision, Writing – review & editing. **Ana M. García-Campaña:** Conceptualization, Supervision, Writing – review & editing, Project administration, Funding acquisition. **Gaud Dervilly:** Conceptualization, Supervision, Writing – review & editing, Project administration, Funding acquisition.

Data availability

The authors are unable or have chosen not to specify which data has been used.

Acknowledgments

LCR thanks the International Mobility Program Erasmus+ for PhD students (University of Granada, 2020). This project has received funding from the European Union's Horizon 2020 research and innovation programme under the Marie Skłodowska-Curie grant agreement HAZARDOmics No 795946. This study has been funded by MCIN/AEI/ 10.13039/501100011033, through the project PID2021-127804OB-I00 (Co-funded by European Regional Development Fund - ERDF, a way to build Europe).

Supplementary materials

Supplementary material associated with this article can be found, in the online version, at doi:10.1016/j.chroma.2022.463502.

References

[1] R. Mukhopadhyay, IMS/MS: its time has come, Anal. Chem. 80 (2018) 7918–7920.
[2] E. Charles, K. Thalassinos, Developments in tandem ion mobility mass spectrometry, Biochem. Soc. Trans. 48 (2020) 2457–2466, doi:10.1042/BST20190788.
[3] C. Lapthorn, F. Pullen, B.Z. Chowdhry, Ion mobility spectrometry-mass spectrometry (IMS-MS) of small molecules: separating and assigning structures to ions, Mass Spectrom. Rev. 32 (2013) 43–71, doi:10.1002/mas.21349.
[4] F. Lanucara, S.W. Holman, C.J. Gray, C.E. Eyers, The power of ion mobility-mass spectrometry for structural characterization and the study of conformational dynamics, Nat. Chem. 6 (2014) 281–294, doi:10.1038/nchem.1889.
[5] T. Mairinger, T.J. Causon, S. Hann, The potential of ion mobility-mass spectrometry for non-targeted metabolomics, Curr. Opin. Chem. Biol. 42 (2018) 9–15, doi:10.1016/j.cbpa.2017.10.015.
[6] G. Paglia, J.P. Williams, L. Menikarachchi, J.W. Thomposon, et al., Ion mobility derived collision cross sections to support metabolomics applications, Anal. Chem. 86 (2014) 3985–3993, doi:10.1021/ac500405x.
[7] W. Vautz, D. Zimmermann, M. Hartmann, J.I. Baumbach, et al., Ion mobility spectrometry for food quality and safety, Food Add. Contam. 23 (2016) 1064–1073, doi:10.1080/02652030600889590.
[8] M. Hernández-Mesa, D. Ropartz, A.M. García-Campaña, H. Rogniaux, et al., Ion mobility spectrometry in food analysis: principles, current applications and future trends, Molecules 24 (2019) 2706, doi:10.3390/molecules24152706.
[9] M. Hernández-Mesa, A. Escourrou, F. Monteau, B.Le Bizec, G. Dervilly-Pinel, Current applications and perspectives of ion mobility spectrometry to answer chemical food safety issues, TrAC. Trends Anal. Chem. 94 (2017) 39–53, doi:10.1016/j.trac.2017.07.006.
[10] V. D'Atri, T. Causon, O. Hernandez-Alba, A. Mutabazi, et al., Adding a new separation dimension to MS and LC-MS: what is the utility of ion mobility spectrometry? J. Sep. Sci. 41 (2018) 20–67, doi:10.1002/jssc.201700919.
[11] L. Ahonen, M. Fasciotti, G. Boije af Gennäs, T Kotiaho, et al., Separation of steroid isomers by ion mobility mass spectrometry, J. Chromatogr. A 1310 (2013) 133–137, doi:10.1016/j.chroma.2013.08.056.
[12] A.B. Kanu, P. Dwivedi, M. Tam, L. Matz, H.H. Hill, Ion mobility–mass spectrometry, J. Mass Spectrom. 43 (2008) 1–22, doi:10.1002/jms.1383.
[13] R. Cumeras, E. Figueras, C.E. Davis, J.I. Baumbach, I. Gràcia, Review on ion mobility spectrometry. Part : current instrumentation, Analyst 140 (2015) 1376–1390, doi:10.1039/C4AN01100G.
[14] H.E. Revercomb, E.A. Mason, Theory of plasma chromatography/gaseous electrophoresis—a review, Anal. Chem. 47 (1975) 970–983, doi:10.1021/ac60357a043.
[15] J.A. Picache, B.S. Rose, A. Balinski, K.L. Leaptrot, et al., Collision cross section compendium to annotate and predict multi-omic compound identities, Chem. Sci. 10 (2019) 983–993, doi:10.1039/C8SC04396E.
[16] M. Hernández-Mesa, B.L. Bizec, F. Monteau, A.M. García-Campaña, G. Dervilly-Pinel, Collision Cross Section (CCS) database: an additional measure to characterize steroids, Anal. Chem. 90 (2018) 4616–4625, doi:10.1021/acs.analchem.7b05117.
[17] J. Regueiro, N. Negreira, M.H.G. Berntssen, Ion-mobility-derived collision cross section as an additional identification point for multiresidue screening of pesticides in fish feed, Anal. Chem. 88 (2016) 11169–11177, doi:10.1021/acs.analchem.6b03381.
[18] J. Regueiro, N. Negreira, R. Hannisdal, M.H.G Berntssen, Targeted approach for qualitative screening of pesticides in salmon feed by liquid chromatography coupled to traveling-wave ion mobility/quadrupole time-of-flight mass spectrometry, Food Control 78 (2017) 116–125, doi:10.1016/j.foodcont.2017.02.053.
[19] S. Goscinny, M. McCullagh, J. Far, E. De Pauw, G. Eppe, Towards the use of ion mobility mass spectrometry derived collision cross section as a screening approach for unambiguous identification of targeted pesticides in food, Rapid Commun. Mass Spectrom. 33 (2019) 34–48, doi:10.1002/rcm.8395.
[20] Y. Fan, F. Liu, W. He, Q. Qin, D. Hu, et al., Screening of multi-mycotoxins in fruits by ultra-performance liquid chromatography coupled to ion mobility quadrupole time-of-flight mass spectrometry, Food Chem. 368 (2022) 130858, doi:10.1016/j.foodchem.2021.130858.
[21] M. McCooeye, B. Kolakowski, J. Boison, Z. Mester, Evaluation of high-field asymmetric waveform ion mobility spectrometry mass spectrometry for the analysis of the mycotoxin zearalenone, Anal. Chim. Acta 627 (2008) 112–116, doi:10.1016/j.aca.2008.05.045.
[22] A. Sheibani, M. Trabrizchi, H.S. Ghaziaskar, Determination of aflatoxins B1 and B2 using ion mobility spectrometry, Talanta 75 (2008) 233–238, doi:10.1016/j.talanta.2007.11.006.
[23] L. Righetti, A. Bergmann, G. Galaverna, O. Rolfsson, G. Paglia, C. Dall'Asta, Ion mobility-derived collision cross section database: application to mycotoxin analysis, Anal. Chim. Acta 1014 (2018) 50–57, doi:10.1016/j.aca.2018.01.047.
[24] L. Righetti, M. Fenclova, L. Dellafiora, J. Hajslova, M. Stranska-Zachariasova, C. Dall'Asta, resolution-ion mobility mass spectrometry as an additional powerful tool for structural characterization of mycotoxin metabolites, Food Chem. 245 (2018) 768–774, doi:10.1016/j.foodchem.2017.11.113.
[25] L. Righetti, N. Dreolin, A. Celma, A.M. McCullagh, et al., Travelling wave ion mobility-derived collision cross section for mycotoxins: investigating interlaboratory and interplatform reproducibility, J. Agri. Food Chem. 68 (2020) 10937–10943, doi:10.1021/acs.jafc.0c04498.
[26] P.L. Schiff, Ergot and its alkaloids, Am. J. Pharm. Educ. 70 (2006) 98, doi:10.5688/aj700598.
[27] K.M. Hines, D.H. Ross, K.L. Davidson, M.F. Bush, L. Xu, Large-scale structural characterization of drug and drug-like compounds by high-throughput ion mobility-mass spectrometry, Anal. Chem. 89 (2017) 9023–9030, doi:10.1021/acs.analchem.7b01709.
[28] R. Krska, C. Crews, Significance, chemistry and determination of ergot alkaloids: a review, Food Addit. Contam.: Part A 25 (2008) 722–731, doi:10.1080/02652030701765756.
[29] D. Arcella, J.A. Gómez-Ruiz, M.L. Innocenti, R. Roldán, Scientific Report: human and animal dietary exposure to ergot alkaloids, EFSA J. 15 (2017) 4902, doi:10.2903/j.efsa.2017.4902.
[30] P.M. Scott, Ergot alkaloids: extent of human and animal exposure, World Mycotoxin J. 2 (2009) 141–149, doi:10.3920/WMJ2008.1109.
[31] European Commission, Commission Recommendation of 15 March 2012 on the monitoring of the presence of ergot alkaloids in feed and food, Off. J. EU 77 (2012) 20–21.
[32] EFSA. Panel on Contaminants in the Food Chain (CONTAM), Scientific Opinion on Ergot alkaloids in food and feed, EFSA J. 10 (2012) (2012) 158, doi:10.2903/j.efsa.2012.2798.
[33] European Commission, Commission regulation (EU) 2021/1399 of 24 August 2021 amending Regulation (EC) No 1881/2006 as regards maximum levels of ergot sclerotia and ergot alkaloids in certain foodstuffs, Off. J. EU 301 (2021) 1–5.
[34] N. Arroyo-Manzanares, L. Gámiz-Gracia, A.M García-Campaña, J. Diana di Magunvu, S. De Saeger, Ergot alkaloids: chemistry, biosynthesis, bioactivity, and methods of analysis, in: J.M. Mérillon, K. Ramawat (Eds.), Fungal Metabolites, Springer International Publishing Switzerland, 2016, pp. 1–43.
[35] C. Crews, Analysis of ergot alkaloids, Toxins 7 (2015) 2024–2050, doi:10.3390/toxins7062024.
[36] S.A. Tittlemier, B. Cramer, C. Dall'Asta, M.H. Iha, V.M.T. Lattanzio, et al., Developments in mycotoxin analysis: an update for 2018–2019, World Mycotoxin J. 13 (2020) 3–24, doi:10.3920/WMJ2019.2535.
[37] Skyline Software 21.1 (2021) Retrieved from https://skyline.ms/project/home/begin.view. (Accessed on 15 July 2021).
[38] L. Carbonell-Rozas, L. Gámiz-Gracia, F.J. Lara, A.M. García-Campaña, Determination of the main ergot alkaloids and their epimers in oat-based functional foods by ultra-high performance liquid chromatography tandem mass spectrometry, Molecules 26 (2021) 3717, doi:10.3390/molecules26123717.
[39] L. Carbonell-Rozas, C.K. Mahdjoubi, N. Arroyo-Manzanares, A.M. García-Campaña, L. Gámiz-Gracia, Occurrence of ergot alkaloids in barley and wheat from Algeria, Toxins 13 (2021) 316, doi:10.3390/toxins13050316.
[40] V. Gabelica, A.A. Shvartsburg, C. Afonso, P. Barran, J.L.P. Benesch, Recommendations for reporting ion mobility mass spectrometry measurements, Mass Spectrom. Rev. 38 (2019) 291–320, doi:10.1002/mas.21585.
[41] C. Tejada-Casado, M. Hernández-Mesa, F. Monteau, F.J. Lara, M del Olmo-Iruela, et al., Collision cross section (CCS) as a complementary parameter to characterize human and veterinary drugs, Anal. Chim. Acta 1043 (2018) 52–63, doi:10.1016/j.aca.2018.09.065.
[42] M. Hernández-Mesa, V. D'Atri, G Barknowitz, M. Fanuel, J. Pezzatt, et al., Interlaboratory and interplatform study of steroids collision cross section by traveling wave ion mobility spectrometry, Anal. Chem. 92 (2020) 5013–5022, doi:10.1021/acs.analchem.9b05247.
[43] M.L. Feuerstein, M. Hernández-Mesa, Y. Valadbeigi, B.L. Bizec, S. Hann, G. Dervilly, T. Causon, Critical evaluation of the role of external calibration strategies for IM-MS, Anal. Bioanal. Chem. (2022), doi:10.1007/s00216-022-04263-5.
[44] N.L. Zakharova, C.L. Crawford, B.C. Hauck, J.K. Quinton, J.K.W.F. Seims, et al., An assessment of computational methods for obtaining structural information of moderately flexible biomolecules from ion mobility spectrometry, J. Am. Soc. Mass Spectrom. 23 (2012) 792–805, doi:10.1007/s13361-012-0339-5.
[45] J. Graton, M. Hernández-Mesa, S. Normand, G. Dervilly, J.Y. Le Questel, B.L. Bizec, Characterization of steroids through collision cross sections: contribution of quantum chemistry calculations, Anal. Chem. 92 (2020) 6034–6042, doi:10.1021/acs.analchem.0c00357.
[46] G. Paglia, M. Kliman, E. Claude, S. Geromanos, et al., Applications of ion-mobility mass spectrometry for lipid analysis, Anal. Bioanal. Chem. 407 (2015) 4995–5007, doi:10.1007/s00216-015-8664-8.
[47] Z. Zhou, J. Tu, Z.J. Zhu, Advancing the large-scale CCS database for metabolomics and lipidomics at the machine-learning era, Curr. Opin. Chem. Biol. 42 (2018) 34–41, doi:10.1016/j.cbpa.2017.10.033.
[48] Z. Zhou, X. Shen, J. Tu, Z.J. Zhu, Large-scale prediction of collision cross-section values for metabolites in ion mobility-mass spectrometry, Anal. Chem. 88 (2016) 11084–11091, doi:10.1021/acs.analchem.6b03091.
[49] L. Bijlsma, R. Bade, A. Celma, L. Mullin, G. Cleland, et al., Prediction of collision cross-section values for small molecules: application to pesticide residue analysis, Anal. Chem. 89 (2017) 6583–6589, doi:10.1021/acs.analchem.7b00741.
[50] CCS base (15 July 2021) Retrieved from https://ccsbase.net/predictions/. (Accessed on 15 July 2021).
[51] AllCCS (15 July 2021) Retrieved from http://allccs.zhulab.cn/. (Accessed on 15 July 2021).
[52] V. Ianchis, M. Gioioso, J. Ballantyne, J.P.C. Vissers, Modular, machine learning-based, multi chemical class CCS prediction pipeline, Poster Note, Waters Corporation, 2020.
[53] V. Domalain, M. Hubert-Roux, V. Tognetti, L. Joubert, C.M. Lange, et al., Enantiomeric differentiation of aromatic amino acids using traveling wave ion mobility-mass spectrometry, Chem. Sci. 5 (2014) 3234, doi:10.1039/C4SC00443D.

[54] T.J. Causon, S. Hann, Theoretical evaluation of peak capacity improvements by use of liquid chromatography combined with drift tube ion mobility-mass spectrometry, J. Chromatog. A 1416 (2015) 47–56, doi:10.1016/j.chroma.2015.09.009.
[55] M. McCullagh, K. Giles, K. Richardson, S. Stead, M. Palmer, Investigations into the performance of travelling wave enabled conventional and cyclic ion mobility systems to characterize protomers of fluoroquinolone antibiotic residues, Rapid Com. Mass Spectrom. 33 (2019) 11–21, doi:10.1002/rcm.8371.
[56] L. Beucher, G. Dervilly-Pinel, S. Prévost, F. Monteau, B.L. Bizec, Determination of a large set of β-adrenergic agonist in animal matrices based on ion mobility and mass separations, Anal. Chem. 87 (2015) 9234–9242, doi:10.1021/acs.analchem.5b01831.
[57] M. Hernández-Mesa, F. Monteau, B.L. Bizec, G. Dervilly-Pinel, Potential of ion mobility-mass spectrometry for both targeted and non-targeted analysis of phase II steroid metabolites in urine, Anal.Chim. Acta: X 1 (2019) 100006, doi:10.1016/j.acax.2019.100006.
[58] H.H. Hill, G. Simpson, Capabilities and limitations of ion mobility spectrometry for field screening applications, Field Anal. Chem. Technol. 1 (1997) 119–134, doi:10.1002/(SICI)1520-6521(1997)1:3⟨119::AID-FACT2⟩3.0.CO;2-S.
[59] M. Kokkonen, M. Jestoi, Determination of ergot alkaloids from grains with UPLC-MS/MS, J. Sep Sci. 33 (2010) 2322–2327, doi:10.1002/jssc.201000114.
[60] S.A Tittlemier, D. Drul, M. Roscoe, T. McKendry, Occurrence of ergot and ergot alkaloids in western canadian wheat and other cereals, J. Agri. Food Chem. 63 (2015) 6644–6650, doi:10.1021/acs.jafc.5b02977.
[61] SANTE/12682/2019. Guidance document on analytical quality control and validation procedures for pesticide residues analysis in food and feed. Implemented by 01.01.2020. European Commission, Health & Consumer Protection Directorate-General, 2–44.
[62] European Commission. Commission Decision (2021/808) of 22 March 2021 on the performance of analytical methods for residues of pharmacologically active substances used in food-producing animals and on the interpretation of results as well as on the methods to be used for sampling and repealing Decisions 2002/657/EC and 98/179/EC, Off. J. EU. 180 (2021) 84–109 http://data.europa.eu/eli/reg_impl/2021/808/oj. (Accessed on 15 January 2022).
[63] K.M. Hines, D.H. Ross, K.L. Davidson, M.F. Bush, L. Xu, Large-scale structural characterization of drug and drug-like compounds by high-throughput ion mobility-mass spectrometry, Anal. Chem. 89 (17) (2017) 9023–9030, doi:10.1021/acs.analchem.7b01709.
[64] CCS base. (2021) Retrieved from https://ccsbase.net/predictions/. [Accessed May 15, 2021].
[65] AllCCS. (2021) Retrieved from http://allccs.zhulab.cn/. [Accessed May 15, 2021].